Catal Lett (2009) 127:113–118
DOI 10.1007/s10562-008-9653-8

# Density Functional Study of the Effects of Strains on the Adsorption of Methoxide and its Decomposed Intermediates on Cu(100) Surface

**Agnes S. Y. Foo · Kok Hwa Lim**

Received: 14 July 2008 / Accepted: 9 September 2008 / Published online: 25 September 2008


**Abstract** Periodic density functional slab models were used to investigate adsorption of methoxide and its decomposed intermediates on optimized and strained (−5% to +5%) Cu(100) surfaces. Surface relaxation energies and adsorption energies of methoxide and its decomposed intermediates were systematically studied and quantified. Reaction energetics of methoxide C–H and C–O bond breaking were quantified on the strained Cu(100) surfaces.

**Keywords** DFT · Adsorption · Methoxide · Decomposition · Cu(100)

## 1 Introduction

Worsening environmental conditions brought about by the emission of greenhouse gases and air pollutants from the use of combustion engines have motivated intensive research on cleaner energy sources. Hydrogen fuel cells, being environmentally friendly, qualify as an excellent candidate over combustion engines [1]. Although $H_2$ is an attractive alternative to fossil fuels, it does not occur as a fuel naturally. Instead, it is found in chemical compounds such as hydrocarbons, from which it must be chemically modified to yield $H_2$. Examples of hydrogen-containing compounds include: natural gas, ethanol and methanol. Methanol can be readily converted into hydrogen at moderate temperatures and a typical process is methanol steam reforming (MSR): $CH_3OH + H_2O \rightarrow H_2 + CO_2$. MSR is considered to be an attractive option for producing hydrogen in situ for on board fuel cells as it is cost effective and easy to handle [2]. The common catalyst for this reaction is Cu/ZnO [1], with its active component attributed by Cu [3]. Experimental findings [4] have suggested that ZnO is unreactive and that the MSR activity of a ZnO-free catalyst is similar to those with ZnO. Near complete conversion can be attained at temperature above 473 K and at high pressure.

MSR is believed to begin with adsorbed methoxide ($CH_3O$), which decomposes further [5]. The direction in which it the reaction proceeds can follow two pathways, and they are: (i) C–H bond breaking which leads to the formation of $CH_2O$ and H and (ii) C–O bond scission, which produces $CH_3$ and O [6–17]. The pathway undertaken depends on the catalyst composition, surface morphology and defects present on the catalysts. The methoxide C–H bond breaking process is widely believed to be the rate determining step of methanol steam reforming [12].

Recent studies have shown that surface strains can have significant effects on the reactivity of transition metal surfaces [18–20], in particular, the binding energy of adsorbates, reaction and activation energies for bond breaking and bond formation occurrences [19, 21]. Interdependent factors like reaction energetics and species surface concentration exert influence on each other in such a way that it can result in an alteration of intermediates' binding energies [22].

The focus of this study is thus to investigate how surface strains affect the adsorption complexes of methoxide and its decomposed intermediates on Cu (100) surface and the overall thermodynamics effects on methoxide C–H and C–O of bond breaking reactions. For the current work, we

A. S. Y. Foo · K. H. Lim (✉)
Division of Chemical and Biomolecular Engineering,
School of Chemical and Biomedical Engineering,
Nanyang Technological University, 62 Nanyang Drive,
Singapore 637459, Singapore
e-mail: kokhwa@ntu.edu.sg

have chosen the Cu(100) surface as a model for the Cu-based catalysts for its simplicity in illustration of the effects. Although true catalysts feature complicated surface structures, it is nevertheless useful to study the elementary reaction steps for idealized model systems, if only for reference purpose [23].

The article is organized as follows. In sect. 2, the computational methods and models are presented. In sect. 3, we discuss the adsorption and reaction energetics of methoxide and its decomposed intermediates on Cu substrates. Finally, we conclude our finding in the last section.

## 2 Computational Methods and Models

All calculations were performed with the plane-wave based Vienna ab initio simulation package [24–26] using the PBE generalized-gradient approximation for the exchange-correlation functional [27]. The interaction between atomic cores and electrons was described by the projector augmented wave method [28]. For integrations over the Brillouin zone, we combined a $3 \times 3 \times 1$ Monkhorst-Pack grid [29]. Throughout, we adopted an energy cut-off of 400 eV, which guarantees good convergence of binding energies from previous studies [12–16]. Coordinates of adsorbates and substrate atoms included in the optimization procedure were optimized until the forces acting on them were less than 0.1 eV/nm.

Extended surfaces of Cu(100) were modeled by four-layer slabs. The unit cells consist of nine atoms per layer to enable us to consider surface coverage as low as 1/9. The periodically repeated slabs are separated by a vacuum spacing of $\sim$1 nm. For adsorption studies, the adsorbates were positioned on one side of the slab. We have studied adsorption on three high symmetry adsorption sites: top, bridge, and hollow (see Fig. 1). The adsorption complexes were studied with relaxation together with the top 2 layers of the substrates while keeping the bottom 2 layers fixed. Binding energy (BE) of an adsorbate is calculated as follows: $\mathrm{BE} = E_{\mathrm{ad}} + E_{\mathrm{sub}} - E_{\mathrm{ad/sub}}$, where $E_{\mathrm{ad/sub}}$ is the total energy of the slab model covered with the adsorbate, and $E_{\mathrm{ad}}$ and $E_{\mathrm{sub}}$ are the total energies of the adsorbate in the gas phase and of the clean substrate, respectively. From this definition, a positive value implies a release of energy or a favorable adsorption.

## 3 Results and Discussion

### 3.1 Optimized and Reconstructed Cu(100) Surfaces

The optimized lattice constant (LC) of Cu bulk structure was calculated to be 3.63 Å. Compressive and expansive strain were introduced parallel to the surface plane of Cu(100) surface by varying the LC in percentage with respect to the bulk optimized LC (0%), ranging from −5% (3.44 Å), −3% (3.52 Å), −1% (3.59 Å), 1% (3.66 Å), 3% (3.73 Å), and 5% (3.81 Å). This method has been previously justified to be able to capture the main effects of strain on transition metal activities [20, 30, 31]. Since artificial strain has been introduced into the Cu substrate, it is institutive to look at the surface relaxation energies of these strained surfaces and the geometries of these reconstructed surfaces. The relative changes in substrate energy with respect to the optimized bulk truncated Cu(100) surface and their corresponding optimized Cu–Cu bond distances were presented in Table 1.

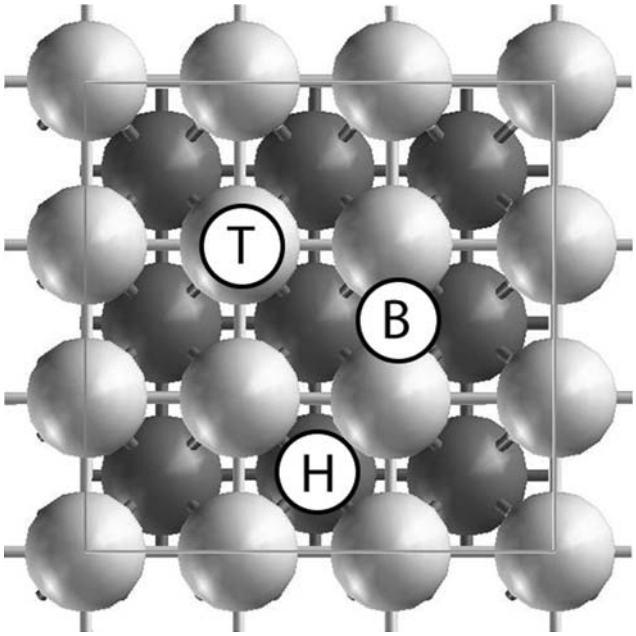


**Fig. 1** Top view of Cu(100) surface unit cell with high symmetry adsorption sites—Top (T), bridge (B), and hollow (H). Light grey sphere—top layer Cu atoms and dark grey sphere—second layer Cu atoms

Our calculations show that a slightly compressed Cu structure (−1% variation in LC) is the most favorable with stabilization energy of −0.004 eV/Cu atom in comparison to the optimized bulk truncated Cu(100) surface. This is likely due to the ability of the Cu atoms to reconstruct the surface leading to optimal Cu–Cu distances of 2.54 Å for the surface Cu and 2.55 Å between top and second layer Cu atoms which is similar to the optimized bulk Cu–Cu bond distance.

While compressive strain of −3% yield a structure of similar stability compared to those with the optimized bulk truncated Cu(100) surface (see Table 1), further compressive strain on the Cu surface destabilized the structure leading to an energy change of 0.028 eV/Cu atom for Cu surface with −5% strain. In contrast, slight expansive

**Table 1** Energy differences per Cu atom between strained and optimized bulk truncated Cu(100) surfaces (top 2 Cu layers have been relaxed), Cu–Cu bond distances between surface layers Cu atoms, (($r_{Cu-Cu}(1)$) and surface layer and second layer Cu atoms of the respective Cu(100) surfaces

| ΔLC (%)[a] | $\Delta E_{substrate}$ (eV/atom) | $r_{Cu-Cu}(1)$ (Å) | $r_{Cu-Cu}(2)$ (Å) |
|---|---|---|---|
| −5 | 0.028 | 2.44 | 2.56 |
| −3 | 0.000 | 2.49 | 2.55 |
| −1 | −0.004 | 2.54 | 2.55 |
| 0 | 0.000 | 2.56 (2.55[b]) | 2.54 |
| +1 | 0.009 | 2.59 | 2.54 |
| +3 | 0.037 | 2.64 | 2.53 |
| +5 | 0.073 | 2.69 | 2.51 |

[a] Variation of lattice constant (LC) with respect to "0"—optimized bulk Cu lattice constant

[b] Optimized bulk truncated Cu–Cu bond distance

strain of +1% already destabilized the Cu surface with energy changes of 0.009 eV/Cu atom. An increase in energy is required for further expansive strain of the Cu surface and 0.073 eV/Cu atom is required for expending the LC by +5%. It is worthy to note that these restructuring energies are relatively small, and we would thus expect that under dynamic catalytic reaction conditions, the Cu surface is dynamic and would be able to reconstruct leading to changes in catalytic activities of the materials.

### 3.2 Atomic H Adsorption

From our calculations, atomic H binds preferably to the highly coordinated site, i.e., hollow site with binding energy of 2.44 eV on the unstrained surface (0%), in agreement with previous finding that H atom preferred hollow sites on the Cu(111) surface with binding energy of 2.46 eV [12]. However, the hollow site is only about 0.5 eV more stable than the most unfavorable top site and hence the H atom is expected to be very mobile on the Cu surface [12]. Similar trend is observed on all the strained surfaces with energy differences between the top site and hollow site differs by at most 0.6 eV (see Table 2). From our calculations, we find that atomic H binds more strongly on the compressive strained Cu(100) surface (ΔLC: −1%, −3%, and −5%) and H atom binds more weakly to the expansive strain Cu(100) surfaces (ΔLC: 1%, 3%, and 5%) in comparison with the bulk optimized LC (see Table 2). In general, except for +5% strained Cu(100) surface, atomic H binding energies at the top, bridge and hollow sites decreases with increases LC (see Table 2). This difference in binding energy can be explained by the optimal covalent bond distance (1.75 Å) between Cu (covalent radii = 1.38 Å) and H (covalent radii = 0.37 Å)

**Table 2** Atomic H binding energies (BE) in eV on various Cu (100) surfaces

| ΔLC (%) | Adsorption sites | | |
|---|---|---|---|
| | Top | Bridge | Hollow |
| −5 | 1.94 | 2.37 | 2.54 |
| −3 | 1.93 | 2.37 | 2.51 |
| −1 | 1.92 | 2.37 | 2.48 |
| 0 | 1.90 | 2.35 | 2.44 |
| +1 | 1.88 | 2.34 | 2.41 |
| +3 | 1.84 | 2.32 | 2.36 |
| +5 | 1.87 | 2.34 | 2.37 |

atoms [32]. As observed in Table 2, the contraction of Cu–Cu bond distances favors better bonding between H atom and the surface Cu atoms (i.e., shorter Cu–H bond distance) and hence leading to stronger interaction between H and the Cu(100) surface in comparison to expanding the surface where stretched Cu–Cu bonds lead to longer H–Cu bond distances and hence weakening the interaction between atomic H and the Cu(100) surface. At ΔLC = 5%, the break in trend can be rationalized by the weakened Cu–Cu interaction due to longer Cu–Cu bond distances and hence lead to a slightly stronger H–Cu bond.

### 3.3 Atomic O Adsorption

From our calculations, atomic O also prefers to bind to highly coordinated site (i.e., hollow site) with binding energy of 5.40 eV on the unstrained Cu(100) surface. This is in agreement with previous finding that O atom preferred hollow sites on the Cu(111) surface [12]. However, the potential energy surface (PES) for the O atom is more corrugated compared to the H atom with energy differences of 1.87 eV between the top site and hollow site on the unstrained Cu(100) surface. This is in agreement with the reported 1.73 eV [12] energy differences between the top site and hollow site on Cu(111) surface bearing in mind that a different GGA (PW91 [12] vs PBE) was used. In contrast to H atom, expansive strain on the Cu(100) surface increases the atomic O binding energies. We observed that binding energies of atomic O increase to 5.51 eV for a +5% strain and decrease to 5.30 eV for a −5% strain on the hollow site (see Table 3). This is because when O adsorbed on the surface, the O atom obtained negative charges from the Cu(100) surface. These negatively charged O atoms are repulsive and hence are stabilized by larger LC leading to the observed adsorption complex stabilization with increase LC. This situation is very similar to the reported case for subsurface C on the Pd(111) surface where stabilization of atomic subsurface C was observed when the 3 × 3 unit cell is increased to a 4 × 4 unit cell [33].

**Table 3** Binding energies in eV of O, $CH_3$, $CH_2O$, and $CH_3O$ at their most favorable adsorption sites

| ΔLC (%) | O Hollow | $CH_3$ Bridge | $CH_2O$ TBT | $CH_3O$ Hollow |
|---|---|---|---|---|
| −5 | 5.30 | 1.45 | 0.16 | 2.38 |
| −3 | 5.34 | 1.45 | 0.21 | 2.42 |
| −1 | 5.39 | 1.46 | 0.25 | 2.45 |
| 0 | 5.40 | 1.44 | 0.26 | 2.45 |
| +1 | 5.43 | 1.44 | 0.27 | 2.45 |
| +3 | 5.50 | 1.44 | 0.29 | 2.48 |
| +5 | 5.51 | 1.51 | 0.29 | 2.46 |

**Table 4** Pertinent geometries of formaldehyde top-bridge–top adsorption complexes on Cu(100) surfaces

| ΔLC (%) | $r_{C–Cu}$ | $r_{O–Cu}$ | $\angle_{Cu–C–O}$ | $\angle_{Cu–O–Cu}$ |
|---|---|---|---|---|
| −5 | 2.19 | 1.99 | 101.1 | 111.6 |
| −3 | 2.18 | 1.98 | 101.5 | 112.9 |
| −1 | 2.17 | 1.98 | 101.6 | 114.7 |
| 0 | 2.17 | 1.98 | 102.1 | 115.1 |
| +1 | 2.16 | 1.98 | 102.2 | 116.1 |
| +3 | 2.15 | 1.98 | 101.8 | 119.0 |
| +5 | 2.16 | 1.97 | 102.9 | 119.4 |

Distances are in Å and angle in degree

### 3.4 Methyl Adsorption

Like on other transition metal surfaces, $CH_3$ binds to Cu substrate via its C atom. From our calculations, $CH_3$ with starting geometry at the hollow site moves to the bridge with binding energy of 1.44 eV (unstrained surface) after optimization. This indicate that on the Cu(100) surface, methyl is not stable at the hollow site. However, the $CH_3$ PES is very flat with energy differences of about 0.1 eV between the top and bridge sites for all the Cu(100) surfaces (varied LC) studied. This is in agreement with previous report that the PES for methyl group is rather flat on Cu surface as well as on other transition metal such as Pd [12]. From our calculations, we observed that there are minimal changes to $CH_3$ binding energies (less than 0.02 eV) on Cu(100) surfaces with varied LC ranging between −5% and +3%, while $CH_3$ is stabilized by about 0.1 eV when ΔLC = +5%. This is likely due to the fact that $CH_3$ prefers the bridge site and hence varying the LC does not lead to significant bonding changes between C and Cu (i.e., $\Delta r_{C–Cu} < 0.02$ Å). It is worthy to note that an expanded surface tends to shorten the $r_{C–Cu}$ bond length. This is due to the weakening of Cu–Cu interactions with increased Cu–Cu bond length which in turn enhanced the interaction between the Cu(100) substrate and $CH_3$.

### 3.5 Formaldehyde Adsorption

Unlike $CH_3$, $CH_2O$ binds to the Cu substrate via both the C and O atoms in the top-bride-top (TBT) adsorption site. This is because, formaldehyde is a close shell molecule and in order to interact with the Cu(100) surface, one of the C–O bonds is weakened to allow both the C and O atoms to interact and form new bonds with the surface Cu atoms. Similar to previous finding [6, 12, 34], our calculations suggest that $CH_2O$ bind very weakly to the Cu substrate with binding energies of about 0.25 eV (see Table 3) for all the Cu(100) surfaces studied (see Table 3). This is in good agreement with previously reported value of 0.11 eV for the $CH_2O$/Cu(111) system using PW91 GGA [12], 0.46 eV for PBE GGA $CH_2O$/Cu(110) [17] system and ∼0.2 eV for $Cu_{22}$ B3LYP/6-31G** cluster model $CH_2O$/Cu(111) system [34]. The slightly higher binding energies obtained here compared to the cu(111) surface [12, 34] is due to the more open and less coordinated surface Cu atoms in agreement when the current result is compared to the more open Cu(110) surface [17]. Here, we observe that expanding the LC, increases the binding energies of $CH_2O$ while compressing LC, destabilizes $CH_2O$ adsorption. This can be rationalized by looking at the geometrical changes of C and O atoms bonding to the surface (see Table 4). At compressed strain of −5%, the $\angle_{Cu–C–O}$ and $\angle_{Cu–O–Cu}$ angles are very strain at 101.1° and 111.6°, respectively. This prevents effective di-$\sigma$ bonding between the C and O atoms with the surface as observed by the longer $r_{C–Cu}$ and $r_{O–Cu}$ bond distance of 2.19 and 1.99 Å, respectively. As the LC of the substrate increases, the strains on $\angle_{Cu–C–O}$ and $\angle_{Cu–O–Cu}$ are gradually reduced as observed with the increase in both $\angle_{Cu–C–O}$ and $\angle_{Cu–O–Cu}$ to 102.9 and 119.4, respectively at LC = +5%. This angle also allow increased di-$\sigma$ interactions between formaldehyde and Cu substrate as observed by the reduction of $r_{C–Cu}$ and $r_{O–Cu}$ bond distance to 2.16 and 1.97 Å, respectively when LC = +5% and hence the increasing trend of binding energies with increase LC.

### 3.6 Methoxide Adsorption

Methoxide is an intermediate of methanol dehydrogenation. Previous configuration interaction calculations on a $Cu_7$ cluster model predicted a binding energy of 2.82 eV for Cu(111) fcc site adsorption, while slab model DFT PW91 calculations show that the binding energy of methoxide at the Cu(111) hollow site is about 2.45 eV. The structure of the $CH_3O$/Cu(111) adsorption complex has also been investigated experimentally [35]. Now, it is generally accepted that methoxide adsorbed at the hollow site with the C–O bond axis oriented perpendicular to the surface. Our

current finding on the Cu(100) surface agrees well with the previous finding on the Cu(111) surface, that is methoxide prefers the highly coordinated hollow site with binding energy of 2.45 eV for the unstrained Cu(100) surface. For adsorption at the top and bridge sites, the binding energies increase almost linearly with expanded LC, similar to the trend observed for atomic O. For the hollow site, methoxide binding energies generally increased with expanded LC except when $\Delta LC = +5\%$ (see Table 3). This is due to the elongation of O–Cu bond from the longer Cu–Cu bond length and hence less effective interaction between methoxide and the Cu(100) surface.

As under dynamic condition, the same amount of energy will be used to create strain on Cu(100) surface and induced changes in the adsorption energies, we shall now study the combine effects of induced surface strain and adsorption energies changes. This effect is summarized in Fig. 2. From Fig. 2, we see that with the combination effects of surface strain and adsorption energies, the most thermodynamics favorable adsorption complexes for all the atoms and molecules studied is when the surface strain is compressive and equals to about $-1\%$. This is mainly due to the favorable exothermic energy released during the relaxation of Cu(100) surface when $LC = -1\%$ compared to the changes in binding energies of the adsorbates.

### 3.7 Energetic of Methoxide C–H and C–O Bond Breaking

The most stable adsorption structure of $CH_3O$ is chosen to represent the initial states for both C–O and C–H bond breaking. The most stable $CH_2O$, $CH_3$, O, and H adsorption complexes are than chosen to be the final state of $CH_3O$ decomposition reactions. To determine how strain affects the reaction pathway, we studied the changes in the C–H and C–O bond breaking reaction energies ($\Delta E$) when strained are applied. The results are summarized in Table 5. Previous studies on transition metal surfaces has showed that changes in $\Delta E$ lead to activation energies changes in the same direction [19, 20] and therefore our current study allow us to have a quantitative analysis of the changes in activation energies from our calculated $\Delta E$.

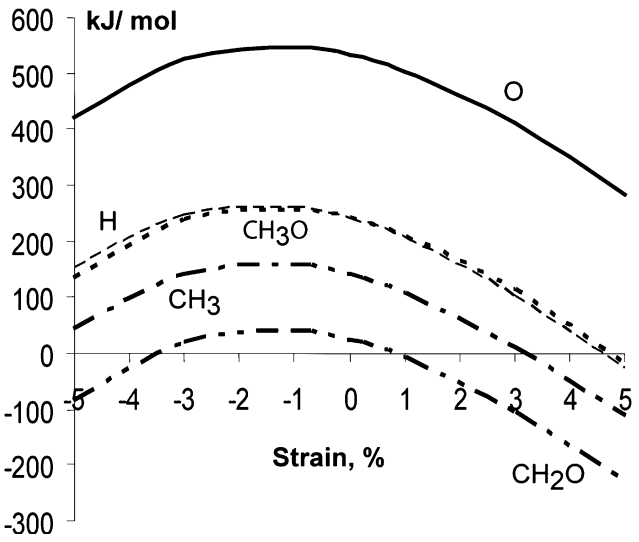


**Fig. 2** Plot of H, O, $CH_3$, $CH_2O$, $CH_3O$ relative binding energies (in eV) of its most favorable adsorption complexes with respect to binding energies at optimized LC on Cu(100) surface vs % changes in LC of Cu(100) surface

**Table 5** Changes in reaction energies ($E_r$) in eV for methoxide C–O[a] and C–H[b] bond breaking reactions

| ΔLC (%) | $E_r$ (C–O) | $E_r$ (C–H) |
|---|---|---|
| −5 | 0.35 | 0.82 |
| −3 | 0.31 | 0.84 |
| −1 | 0.32 | 0.86 |
| 0 | 0.33 | 0.89 |
| +1 | 0.30 | 0.91 |
| +3 | 0.26 | 0.97 |
| +5 | 0.16 | 0.94 |

[a] $CH_3O^* \rightarrow CH_3^* + O^*$

[b] $CH_3O^* \rightarrow CH_2O^* + H^*$

From our calculated $\Delta E$, we see that a compressive strain makes methoxide C–H bond breaking more favorable ($\Delta E = 0.82$ eV, $-5\%$) in comparison to the expansive strain ($\Delta E = 0.94$ eV, $+5\%$). This is in contrast to the methoxide C–O bond breaking reaction where compressive strain makes the reaction less favorable ($\Delta E = 0.35$ eV, $-5\%$) in comparison to the expansive strain ($\Delta E = 0.16$ eV, $+5\%$). With this we would expect the compressive strain Cu(100) to have a higher selectivity for C–H bond breaking path due to reduced activation energies for C–H bond breaking and increased activation energies for C–O bond breaking processes, while an expansive strain Cu(100) surface would lead to a lower selectivity for C–H bond breaking path as it favors C–O bond breaking and disfavors the C–H bond breaking kinetics.

## 4 Conclusion

In this work, we have systematically studied the effects of stain (ΔLC ranging from $-5\%$ to $+5\%$) on the stability of the Cu(100) surfaces. We have also systematically studied the effect of compressive and expansive strain on the binding energies of atomic H, atomic O, methyl, formaldehyde, and methoxide on the Cu(100) surface. In general, atomic H, atomic O and methoxide prefers highly coordinated hollow site, while methyl prefers the bridge site and

formaldehyde prefers to bind to the surface with di-$\sigma$ bonding in the top-bridge-top configuration. We observed that atomic H is stabilized by compressive LC due to better interaction between atomic H and the Cu(100) surface, while expansive LC stabilized the adsorption complexes of atomic O, methyl, formaldehyde and methoxide. The stabilization of the adsorbed species is due to many reasons. Among them, stabilization of atomic O is due to weaker repulsive interaction between the negatively charged O atoms on expanded Cu(100) surface and weaker Cu–Cu interactions that enable stronger adsorbates–substrates interactions.

Previous theoretical studies on transition metal surfaces showed that changes in reaction energies is directly correlated to changes in the activation energies for the particular reaction [19, 20] and therefore form the basis of our current thermodynamic analysis on how strains on the Cu(100) surface affect the reactivity of methoxide C–H and C–O bond breaking reactions. Our calculations revealed that C–H bond breaking is thermodynamically favored on the compressed Cu(100) surface due to greater extend of increased atomic H–Cu(100) surface interactions compared to weaken formaldehyde–Cu(100) interactions. This is in contrast to the expanded Cu(100) surface that favors the C–O bond breaking reactions as the expanded surface favors both the atomic O and methyl interactions with the Cu(100) surface. Therefore, in conclusion, a compressed surface would favor the MSR reaction selectivity as it favors the methoxide C–H bond breaking reactions.

**Acknowledgments** A.S.Y.F. thanks SCBE/NTU FYP projects for financial support. This work was supported by NTUs COE start-up grant M58120016 and SUG 43/06.

## References

1. Trimm DL, Önsan ZI (2001) Catal Rev 43:31
2. Holladay JD, Wang Y, Jones E (2004) Chem Rev 104:4767
3. Günter MM, Ressler T, Jentoft RE, Berns BJ (2001) J Catal 203:133
4. Suwam Y, Ito S, Kameoka S, Tomishige K, Kunimori K (2004) Appl Catal A 267:9
5. Iwasa N, Takezawa N (2003) Top Catal 22:215
6. Lim KH, Chen Z-X, Neyman KM, Rösch N (2006) J Phys Chem B 110:14890
7. Chen J-J, Jiang Z-C, Zhou Y, Chakraborty BR, Winograd N (1995) Surf Sci 328:248
8. Solymosi F, Berko A, Toth Z (1993) Surf Sci 285:197
9. Rebholz M, Kruse NJ (1991) Chem Phys 95:7745
10. Kruse N, Rebholz M, Matolin V, Chuah GK, Block JH (1991) Surf Sci 238:L457
11. Levis RJ, Jiang ZC, Winograd NJ (1988) J Am Chem Soc 110:4431; 111 (1989) 4605
12. Chen Z-X, Neyman KM, Lim KH, Rösch N (2004) Langmuir 20:8068
13. Chen Z-X, Lim KH, Neyman KM, Rösch N (2004) Phys Chem Chem Phys 6:4499
14. Chen Z-X, Lim KH, Neyman KM, Rösch N (2005) J Phys Chem B 109:4568
15. Lim KH, Moskaleva LV, Rösch N (2006) Chem Phys Chem 7:1802
16. Neyman KM, Lim KH, Chen Z-X, Moskaleva LV, Bayer A, Reindl A, Borgmann D, Denecke R, Steinrück H-P, Rösch N (2007) Phys Chem Chem Phys 9:3470
17. Sakong S, Gross A (2007) J Phys Chem A 111:8814
18. Gsell M, Jakob P, Menzel D (1998) Science 280:717
19. Macrikakis M, Hammer B, Norskov JK (1998) Phys Rev Lett 81:2819
20. Grabow L, Xu Y, Mavrikakis M (2006) Phys Chem Chem Phys 8:3369
21. Zhang JL, Vukmirovic MB, Xu Y, Mavrikakis M, Adzic RR (2005) Angew Chem Int Ed 44:2132
22. Kandoi S, Greeley J, Sanchez-Castillo MA, Evans ST, Gokhale AA, Dumesic JA, Mavrikakis M (2006) Top Catal 37:17
23. Somorjai GA (1994) Introduction to surface chemistry and catalysis. Wiley, New York
24. Kresse G, Furthmüller J (1999) Comp Mat Sci 6:15
25. Kresse G, Furthmüller J (1996) Phys Rev B 54:11169
26. Kresse G, Hafner J (1996) Phys Rev B 47:104205
27. Perdew JP, Burke K, Ernzerhof M (1996) Phys Rev Lett 77:3865
28. Kresse G, Joubert D (1999) Phys Rev B 59:1758
29. Monkhorst HJ, Pack JD (1976) Phys Rev B 13:5188
30. Xu Y, Mavrikakis M (2001) Surf Sci 494:131
31. Wintterlin J, Zambelli T, Trost J, Greeley J, Mavrikakis M (2003) Angew Chem Int Ed 42:2850
32. James AM, Lord MP (1992) Macmillan's chemical and physical data. Macmillan, London, UK
33. Lim KH, Neyman KM, Rösch N (2006) Chem Phys Lett 432:184
34. Gomes JRB, Gomes JANF, Illas F (2001) J Mol Catal A: Chem 170:187
35. Amemiya K, Kitajima Y, Yonamoto Y, Terada S, Tsukabayashi H, Yokoyama T, Ohta T (1999) Phys Rev B 59:2307